Article

On-demand, readily degradable Poly-2,3-dihydrofuran enabled by anion-binding catalytic copolymerization

Zhen Zhang[1,2], Wenxiu Lv[1], Maosheng Li[1], Yanchao Wang[1], Xianhong Wang[1,2] ✉ & Youhua Tao [1,2] ✉

Copolymerization with cleavable comonomers is a versatile approach to generate vinyl polymer with viable end-of-life options such as biodegradability. Nevertheless, such a strategy is ineffective in producing readily degradable 2, 3-dihydrofuran (DHF) copolymer with high-molecular-weight (>200 kDa). The latter is a strong and biorenewable thermoplastic that eluded efficient cationic copolymerization synthesis. Here, we show that an anion-binding catalyst seleno-cyclodiphosph(V)azanes enable the efficient cationic copolymerization with cyclic acetals by reversibly activating both different dormant species to achieve both high living chain-end retention and high-molecular-weight. This method leads to incorporating low density of individual in-chain acetal sequences in PDHF chains with high-molecular-weight (up to 314 kDa), imparting on-demand hydrolytic degradability while without sacrificing the thermomechanical, optical, and barrier properties of the native material. The proposed approach can be easily adapted to existing cationic polymerization to synthesize readily degradable polymers with tailored properties while addressing environmental sustainability requirements.

Plastic accumulation has become a substantial environmental crisis[1–3]. As a result, to gain degradable and recyclable plastics for mitigating plastics littering has become an ambitious task over the recent years[4–11]. However, the inert nature of the carbon-carbon backbone in vinyl polymer, which accounts for half of all polymers produced[12,13], has posed a formidable challenge for their degradability or deconstructability[14,15]. As an unusual vinyl polymer, poly-2,3-dihydrofuran (PDHF) has drawn significant research attention[16–20], as it has several environmental benefits, such as oxidative degradability[21], and a bio-based production from 1,4-butanediol[22] (Fig. 1a). In particular, with the advancement of current controlled cationic polymerization system, the PDHF with high-molecular-weight (>250 kg/mol) and excellent property has been achieved under mild conditions[23]. Exceptional strength and toughness, good barrier property, high transmittance are all compelling features of high-molecular-weight PDHF that advocate for its potential adoption. While high-molecular-weight, carbon-

carbon backbone and low oxygen permeability in PDHF contribute to its appealing material qualities, these characteristics are also often commensurate with the decreased degradation rate in the environment. Moreover, the oxidative degradation of PDHF under practical conditions remains notably sluggish[21]. Therefore, designing PDHF with facile degradability while maintaining its attractive properties is of contemporary interest.

One solution to impart facile degradability of PDHF materials entails the copolymerization of DHF with a specialized comonomer through cationic polymerization. While there have been many efforts towards the synthesis of degradable vinyl polymers, via copolymerization approaches[24–34], two significant challenges still exist in current cationic copolymerization systems featuring DHF monomer. First, the homo-polymerization of DHF is extremely rapid compared to the addition of the cleavable comonomers. Accordingly, the generated copolymers contain large strands of DHF homopolymer that suffers

[1]Key Laboratory of Polymer Ecomaterials & State Key Laboratory of Polymer Science and Technology, Changchun Institute of Applied Chemistry, Chinese Academy of Sciences, Changchun, China. [2]University of Science and Technology of China, Hefei, China. ✉e-mail: xhwang@ciac.ac.cn; youhua.tao@ciac.ac.cn
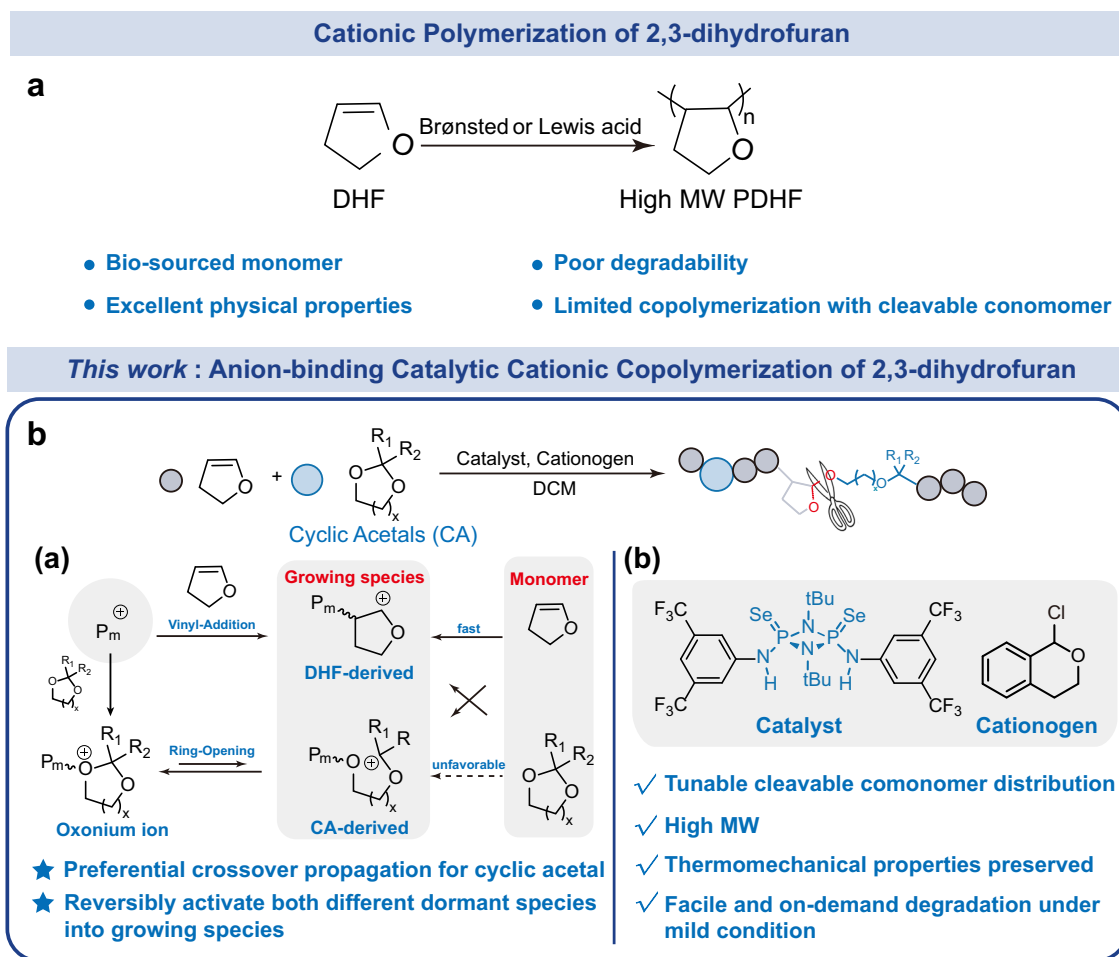
Fig. 1 | Cationic (co)polymerization of DHF. a Cationic polymerization of DHF towards high-molecular-weight PDHF. **b** Proposed anion-binding catalytic cationic copolymerization strategy for synthesizing high-molecular-weight while readily degradable DHF copolymer. Inset: **a** The cationic copolymerization process between DHF and ideal cyclic acetal comonomer. **b** The features of PDHF material produced by anion-binding catalyst.

from poor degradability. Second, control over the molecular weight of copolymer is limited due to the comonomer, which can disturb the reversible-deactivation process, causing chain transfer and chain termination. There is only one report, thus far, by Aoshima, on synthesizing PDHF-based copolymer through copolymerizing DHF with benzaldehyde, yet still suffered from poor control of molecular weight[35].

Recently, we disclosed anion-binding catalysis as an effective approach to address the challenging task in cationic polymerization, in which anion-binding interaction could establish fast reversible-deactivation equilibrium by dynamically binding and dissociating with the counteranions, enabling the precisely controlled polymer structure and chain length[36,37]. Bearing this mechanism in mind, we envisioned designing a high-molecular-weight PDHF material possessing dispersed cleavable groups that allow for the facile degradation, through anion-binding catalytic cationic copolymerization of DHF with cleavable comonomer (Fig. 1b). Cyclic acetals featuring structure simplicity, derived from inexpensive and biorenewable feedstock[38,39], can undergo ring-opening cationic (co) polymerization[34,40–45], resulting in degradable acetal bonds. Aoshima et al., previously demonstrated the cationic copolymerization of cyclic acetals with vinyl ether or styrene via a conventional metal Lewis acid catalytic process[46,47]. Coates et al., have developed elegant strategies for more controlled cationic ring-opening polymerization towards ultra-high-molecular-weight polyacetals[48,49]. Nevertheless, the controlled cationic copolymerization of DHF with cyclic acetals

has remained elusive. Central to the viability of the copolymerization process is judicious selection of the cyclic acetal, which can preferentially add to the growing DHF-derived carbocation while possessing unfavorable propensity to homo-propagation, thus leading to readily degradable PDHF with sparse backbone acetal groups. We further envisioned that the anion-binding interaction may be particularly effective to reversibly activate both different dormant species-such as derived from DHF through vinyl-addition and cyclic acetals through ring-opening, substantially generating long-lived species and thus high-molecular-weight PDHF copolymer. In this work, we demonstrate that anion-binding catalyst enables the highly efficient cationic copolymerization of DHF and cyclic acetals, a long-standing challenge in polymer chemistry. The resulting high-molecular-weight PDHF copolymers exhibit a desirably low acetal content while maintaining the intrinsic material properties of the native polymer, alongside enhanced degradability.

Results

Screening ideal comonomer

We considered that cyclic acetals could serve as ideal comonomer to impart PDHF with facile degradability. Initially, to identify the most suitable comonomer, 1,3-dioxolane (DOL), 1,3-dioxane (DOX) and 1,3-dioxepane (DOP) were selected as model comonomers because of their simplest structures, with seleno-cyclodiphosph(V)azanes **1a** as catalyst and α-chloroisochroman (ICCI) as cationogen in dichloromethane (DCM) at 0 °C (Fig. 2). However, the copolymerization exhibited nearly
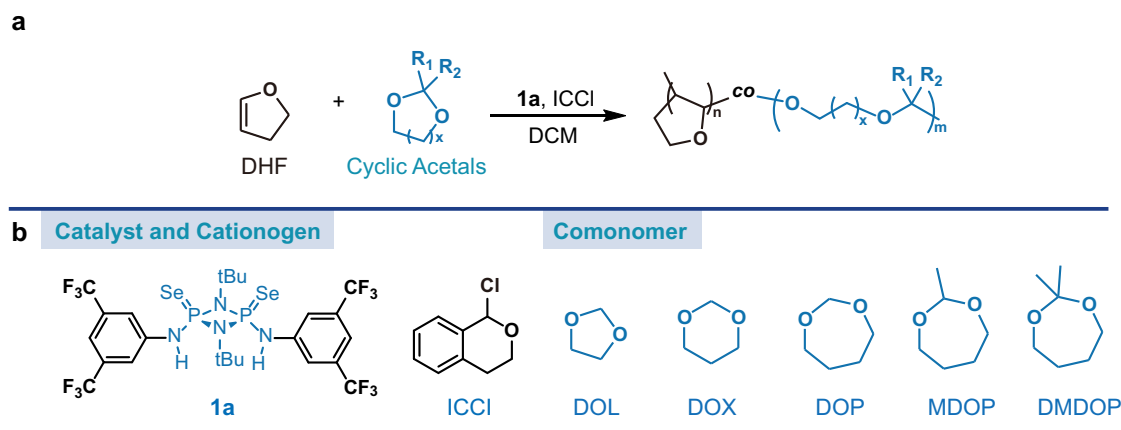
Fig. 2 | Anion-binding catalytic cationic copolymerization of DHF with CA. a Synthesis of PDHF-CA copolymer. **b** The structures of catalyst, cationogen, and comonomers used.

Table 1 | Cationic Copolymerization of DHF with CA[a]

Entry	Comonomer	[DHF]$_0$/[CA]$_0$ /[ICCl]$_0$/[1a]$_0$	Time (h)	DHF/CA Conv.(%)[b]	CA content (%)[c]	$M_{n,calcd}$ (kDa)[d]	$M_{n,SEC}$ (kDa)[e]	Đ (M_w/M_n)[e]
1	DOL	200/200/1/1	2	>99/0	0	14.2	16.2	1.35
2	DOX	200/200/1/1	2	>99/0	0	14.2	17.2	1.32
3	DOP	200/200/1/1	2	>99/2	1	14.6	17.6	1.31
4	MDOP	200/200/1/1	2	>99/28	20	20.6	19.3	1.40
5	DMDOP	200/200/1/1	2	>99/27	18	21.2	4.1	1.83
6[f]	DMDOP	200/200/1/1	2	98/26	20	21.0	18.9	1.33
7[f]	DMDOP	100/100/1/1	0.5	98/27	n.d.[g]	10.4	9.4	1.33
8[f]	DMDOP	100 + 100/100 + 100/ 1/1	0.5 + 1.5	98 + 97/27 + 25	20	20.8	18.4	1.34

[a]Copolymerization conditions: [DHF]$_0$ = [CA] = 1.0 M at 0 °C in DCM; Entries 1-5: Copolymerizations of DHF with different Cyclic Acetals; Entry 6: Polymerizations were carried out at −40 °C; Entries 7-8: Livingness of chain-end was confirmed by sequential monomer addition experiment.
[b]Conversions of DHF and DMDOP were determined by ^{1}H NMR using 1,1,2,2-tetrahydronaphthalene as internal standard.
[c]The CA content in copolymer was calculated by the ^{1}H NMR analysis of product.
[d]$M_{n,calcd}$ = (M_{DHF} × [DHF]$_0$/[ICCl]$_0$× Conv.$_{DHF}$ + M_{CA} × [CA]$_0$/[ICCl]$_0$ × Conv.$_{CA}$) + 133.18.
[e]$M_{n,SEC}$ and Đ were measured by GPC (35 °C, PS standards).
[f]Polymerizations were carried out at −40 °C.
[g]The CA content has not determined.

negligible conversion of these cyclic acetals (Table 1, entry 1–3), and only producing PDHF homopolymer, which could be attributed to the inefficient propagation reaction of these comonomers and exceedingly fast homo-propagation of DHF. Under the homopolymerization condition of [M]$_0$:[ICCl]$_0$:[1a]$_0$ = 200:1:1 at 0 °C in DCM,we observed the extremely slow conversion of cyclic acetals while DHF shows high homopolymerization reactivity (Table S1). Actually, for unsubstituted simple cyclic acetals, activating chain-end by this anion-binding catalyst to generate primary carbocation for propagation is thermodynamically less favorable due to the inherent instability of 1°carbocation and relative weak anion-binding interaction (comparing with metal catalyst), which prohibits further propagation of polymer chain (Fig. S8). We considered the insufficient activation of these acetal-derived chain-ends by anion-binding catalyst and extremely high reactivity of DHF homo-propagation are responsible for only polyDHF homopolymer generated in copolymerization. In order to improve the copolymerizability of comonomers, we attempted to optimize the structure of cyclic acetals based on DOP because the modification on the seven-membered ring wherein presents relatively higher ring strain than five or six-membered ring can potentially promote ring-opening reaction more effectively. In addition, it is well-known that the copolymerizability of cyclic acetals is affected by substituent effect at α-position, which can provide different stabilization to the carbocation species generated via ring-opening of the cyclic acetals oxonium[40,47]. Guided by this, we adopted α-

substitution strategy in the parent DOP monomer. When substituting only one α-hydrogen in DOP with a methyl group, [2-methyl-1,3-dioxepane (MDOP)], the copolymerization indeed proceeded to some extent, but the produced copolymer still contained MDOP-MDOP homo-sequence, which was verified by the two resonance signals of acetal proton at 4.6–5.2 ppm and two methyl signals at 1.25 and 1.15 ppm observed in ^{1}H NMR spectrum (Fig. S4). We considered that the tendency of homo-propagation of MDOP may enable cleavable groups insufficiently spaced out, thus resulting in detrimental effects on the material properties. Compared with MDOP comonomer, substituting both α-hydrogens with methyl groups [2,2-dimethyl-1,3-dioxepane (DMDOP)], exhibits a less pronounced preference for homo-propagation. Indeed, no homopolymerization of DMDOP occurred in the presence of the anion-binding catalyst seleno-cyclodiphosph(V) azanes 1a (Table S1), illuminating the absence of the consecutive DMDOP insertions in DHF copolymerization.^{1}H NMR spectrum of P(DHF-co-DMDOP) copolymer showed the resonance corresponding to the acetal and methyl group at 5.0 and 1.1 ppm for DMDOP, respectively (Fig. 3a), which verified successful insertion of DMDOP into PDHF backbone. The formation of targeted random copolymer is confirmed by the presence of a single diffusion coefficient in Diffusion Ordered Spectroscopy (DOSY NMR) (Fig. 3b). A quick screening on temperature revealed that copolymerization works superbly well at −40 °C, furnishing targeted copolymer not only possessing dispersed cleavable
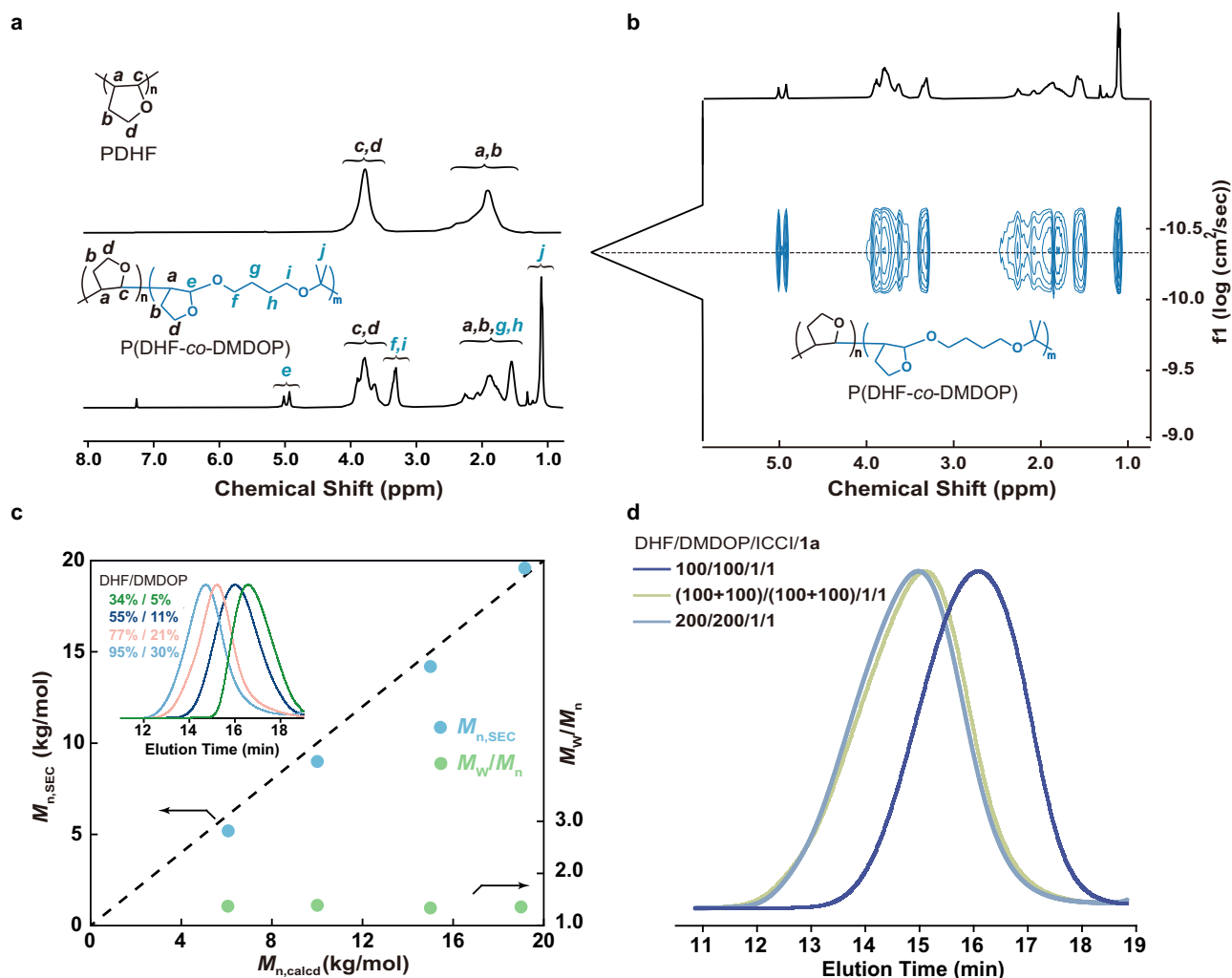
Fig. 3 | Anion-binding catalytic cationic copolymerization of DHF with DMDOP. **a** ^{1}H NMR spectra of PDHF and P(DHF-co-DMDOP) in CDCl$_3$ (Table 1, entry 5). **b** DOSY NMR spectra of P(DHF-co-DMDOP) in CDCl$_3$ (Table 1, entry 5). **c** Polts of $M_{n,SEC}$ and $Đ$ (M_w/M_n) as a function of $M_{n,calcd.}$ (calculated by monomer conversion).

Inset: Overlay of SEC profiles at varied DHF and DMDOP conversions. Copolymerization conditions: [DHF]$_0$:[DMDOP]$_0$:[ICCI]$_0$:[**1a**]$_0$ = 200:200:1:1 at −40 °C in DCM. **d** SEC profiles of the copolymers obtained by sequential monomer addition experiment (Table 1, entry 6-8).

groups but also exhibiting controlled M_n closed to the theoretical value and a low molecular weight distributions ($Đ$ = 1.33) (Table 1, entry 6).

Motivated by the favorable results obtained in the initial screening, we proceeded to thoroughly explore the copolymerization behavior of DHF and DMDOP. Using [DHF]$_0$:[DMDOP]$_0$:[ICCI]$_0$:[**1a**]$_0$ = 200:200:1:1, the copolymerization proceeded smoothly and reached 95% conversion for DHF after 2 hours at −40 °C in DCM (Figs. 3C, S9). $M_{n,SEC}$ grew linearly as a function of monomer conversion and exhibited superior agreement with theoretical M_n (Fig. 3c, Table S2), indicating the copolymerization was mediated by long-lived active species and proceeded in a controllable manner. The chain-end livingness in the DHF-DMDOP copolymerization was further verified through sequential monomer addition (Table 1, entries 7 and 8). Specifically, upon sequential introduction of fresh monomer, SEC analysis of resulting copolymer exhibited a clear shift toward higher molecular weight, while preserving a unimodal molecular weight distribution (Fig. 3d). The reactivity ratios of the two monomers were determined to be r_1 = 4.8, r_{DMDOP} = 0.03 via the Kelen–Tüdõs method[50] (Fig. S10, Table S3). The small product of the reactivity ratios ($r_1 \times r_{DMDOP}$ < 0.15) indicates a moderate degree of monomer alternation in this copolymerization. The even incorporation of facile degradable DMDOP units throughout the polymer chain is highly desired to impede the generation of hardly deconstructable PDHF segments.

Synthesis of high-molecular-weight PDHF copolymer via anion-binding catalysis

In general, by accessing high-molecular-weight PDHF copolymer, we could gain access to a thermoplastic with highly desirable properties. However, the development of efficient polymerization for high-molecular-weight copolymer remains challenge, due to inevitable termination and chain-transfer (Fig. S12), especially at the later stage of polymerization. The anion-binding catalytic mechanism could maintain low cation concentrations, therefore minimizing undesired termination and irreversible chain transfer. We posited that this new method could allow us to target deconstructable PDHF copolymer with high-molecular-weight for the first time.

In this sense, anion-binding catalyst **1a**, was investigated for the copolymerization of DHF and DMDOP in DCM at −40 °C. By varying the ratio of the DHF to DMDOP, we successfully targeted a series of copolymers, P(DHF-DMDOP$_{2.6}$), P(DHF-DMDOP$_{3.6}$), P(DHF-DMDOP$_{6.9}$), P(DHF-DMDOP$_{9.7}$) with M_n value up to 314 kDa (Table 2, entry 1-4). As shown in Table S4, compared with the catalyst substituted by Ph (**1c**) or 3-CF$_3$Ph (**1b**) on seleno-cyclodiphosph(V)azanes framework, the catalyst **1a** (3,5-(CF$_3$)$_2$Ph substituted) shows the higher catalytic reactivity, while **1b** and **1c** hardly produce high-molecular-weight copolymer (catalysis activity: **1a** > **1b** > **1c**). We considered that the electron-withdraw-effect of two CF$_3$ renders catalyst **1a** enhanced multiple strong N-H$_a$--Cl

Table 2 | Synthesis of high-molecular-weight PDHF copolymers and pure PDHF[a]

Entry	Isolated polymer	$[DHF]_0/[CA]_0$	$[DHF]_0/[CA]_0/$ $[ICCl]_0/[1a]_0$	Conv. (%)[b]	CA content (%)[c]	$M_{n,MALLS}$ (kg/mol) [d]	Đ (M_w/M_n) [d]
1	P(DHF-DMDOP$_{2.6}$)	8.0/0.4	8000/400/1/1	92/28	2.6	313.9	1.45
2	P(DHF-DMDOP$_{3.6}$)	8.0/0.8	8000/800/1/1	95/27	3.6	276.1	1.58
3	P(DHF-DMDOP$_{6.9}$)	8.0/1.6	8000/1600/1/2	91/22	6.9	240.4	1.50
4	P(DHF-DMDOP$_{9.7}$)	8.0/2.7	8000/2667/1/3	96/26	9.7	188.5	1.78
5[e]	PDHF	8.0	8000/1/1	92	-	427.9	1.35

[a]Copolymerizations were performed at −40 °C in DCM with $[DHF]_0/[ICCl]_0$ = 8000/1 and different DHF/DMDOP ratios.
[b]Determined by ^{1}H NMR analysis using 1,1,2-tetrahydronaphthalene as internal standard.
[c]The CA content in the copolymer was calculated by the ^{1}H NMR analysis.
[d]$M_{n,MALLS}$, and Đ were measured by SEC multi-angle laser light scattering (MALLS) analysis in THF.
[e]Homopolymerization of DHF at identical conditions.

interaction and weak C-H$_b$---Cl interaction, in which **1a** could act as a quadruple H-bond donor during the binding of anions, thus increasing anion affinity and catalysis activity (Fig. S15). For comparison, the catalyst systems used for controlled polymerization[23] of DHF and copolymerization[44,45] of vinyl ether and cyclic acetals in previous reports were also examined under same condition. When using the anion-binding catalyst tris(3,5-bis(trifluoromethyl)phenyl)thiophosphotriamide **1d** combining cationogen 1,2,3,4,5-pentakis(methoxycarbonyl)cyclopenta-1,3-diene PCCP, a system for controlled polymerization of DHF[23], no conversion of monomer was observed at low temperature (Table S4, entry 8). Subsequent attempts under literature conditions (room temperature) enabled effective copolymerization for this system (Table S4, entry 6), yet attempt to synthesize high-molecular-weight copolymers at high feed ratios still failed (Table S4, entry 7). The catalytic system, for controlled copolymerization of isobutyl vinyl ether (IBVE) and cyclic acetals, combining SnCl$_4$ with lewis base EtOAc showed extremely high reactivity, rendering the thermal runaway ("explosive polymerization"), thus resulting in a low M_n and broad M_w/M_n (Table S4, entry 11). No polymer was obtained when SnCl$_4$/TiCl$_4$/ 1-(isobutoxy)ethyl acetate (IBEA)/EtOAc/ 2,6-di-tert-butylpyridine (DTBP) was used (Table S4, entry 12), a catalytic system for controlled copolymerization of 2-chloroetyl vinyl ether (CEVE) and cyclic acetals. For studies of physicochemical properties, pure PDHF controls were also prepared. Using this anion-binding catalytic system, pure PDHF with M_n up to 428 kDa is achieved (Table 2, entry 5), which is approximately 2 times larger than what has been obtained by previous methods[23].

These results clearly suggest anion-binding catalysis can provide an ideal strategy for accessing deconstructable PDHF copolymer since it enable not only arbitrary conomomer components, but also promotes reversible deactivation of the propagating species to achieve high living chain-end retention and high- molecular-weight.

Copolymer degradation

During the initial stages of developing a new plastic, it's crucial to evaluate the options for degrading the material at its end of life. After formation of PDHF copolymer, which had cleavable acetals along the backbone, the degradation of this copolymer was investigated. In a solution of THF/water (11:1) containing HCl (1.0 M) at room temperature, the PDHF copolymer readily degrades into oligomers as evidenced by SEC (Fig. 4a). For example, the M_n of P(DHF-DMDOP$_{2.6}$) ($M_{n,SEC}$ = 210.5 kg/mol) decreased from 210.5 to 6.9 kg/mol in 10 minutes. Reference experiments with neat PDHF show almost unchanged molecular weight (Figure S20).

To verify the chemical structure of the low-molecular-weight degradation products, purified mixtures obtained through acid hydrolysis of P(DHF-DMDOP$_{6.9}$) (0.25 M HCl) were characterized using ^{1}H NMR and MALDI-TOF-MS. The ^{1}H NMR spectrum of the degradation products revealed minor peaks at 5.0 and 5.4 ppm (designated as e′), as shown in Fig. 4b. These signals indicate the

formation of terminal cyclic hemiacetal structures resulting from acetal bond cleavage. Furthermore, MALDI-TOF-MS analysis provided precise mass data that unambiguously identified end-group structures, confirming the generation of corresponding degradation products expected from acetal hydrolysis (Fig. 4c). However, previous pure PDHF degradation via oxidative pathway exhibited limited control over oligomer architecture and end-group fidelity, given undefined degradation products. The dihydroxyl-terminated PDHF diol may exhibit great potential for further applications, such as synthesis of polyurethane, representing a more sustainable and recyclable route for the end-of-life management of PDHF copolymers. Overall, the high-molecular-weight PDHF copolymer with robust physical properties and on-demand degradation in a predictable manner is highly desired for applications. In addition, the degradation of rectangle-shaped specimens was also performed by immersing into camphorsulfonic acid (CSA) aqueous solution (1.0 M). Complete degradation was observable even under ambient temperature (22–25 °C) within experimentally relevant timeframes (Fig. 4d). The P(DHF-DMDOP$_{2.6}$) sample exhibited significant surface erosion and fragmentation within 30 days. SEC analysis of the 90-day degraded P(DHF-DMDOP$_{2.6}$) showed a molecular weight reduction to M_n of 6.0 kg/mol. In contrast, the neat PDHF control polymer remained intact under identical hydrolysis conditions. We propose that the rapid hydrolytic degradation of the PDHF copolymer arises from the acetal sequences incorporated into the copolymer backbone. These readily cleavable acetal moieties promote backbone hydrolysis under acidic conditions, resulting in chain fragmentation.

To verify the oxidative degradation pathway of the degradation products (low molecular weight PDHF), the oligomers were pulverized to enhance specific surface area and subjected to atmospheric oxygen exposure at 40 °C for environmental degradation assessment. The slightly elevated temperature was employed to enable detectable molecular weight changes within a experimentally practical timeframes. Unfortunately, the degradation products did not exhibit significant molecular weight changes within the limited timeframe (30 days) (Fig. S19). Therefore, accelerated oxidative degradation experiments employing a Fenton reaction system were conducted to demonstrate the possibility of complete degradation of the oligomer at room temperature (-22 °C). Notably, the oligomers exhibited accelerated degradation kinetics under Fenton conditions, demonstrating a progressive 67% molecular weight reduction by day 15 (Fig. 4e and f), which indicated that the degradation products possess ambient oxidative degradability, with degradation rates dependent on specific environmental conditions.

Physical properties of PDHF copolymers

The Differential Scanning Calorimetry (DSC) and thermogravimetric analysis (TGA) were utilized to evaluate the thermal properties of high-molecular-weight PDHF copolymer samples. The T_gs were moderately
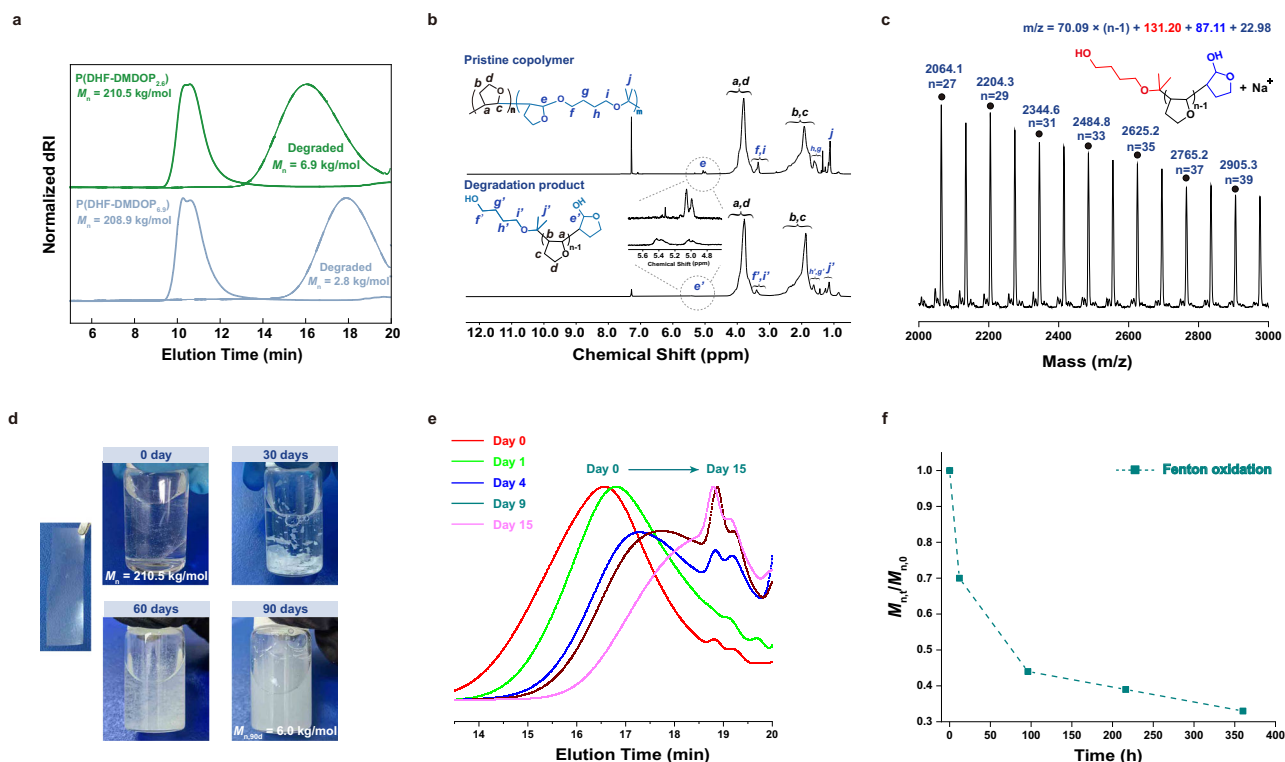
Fig. 4 | The degradation of PDHF copolymer. a The SEC profiles of P(DHF-DMDOP$_{2.6}$) and P(DHF-DMDOP$_{6.9}$) in response to HCl treatment after 10 minutes. **b** ^{1}H NMR spectra of P(DHF-DMDOP$_{6.9}$) and its degradation product after acidic hydrolysis in CDCl$_3$. **c** MALDI-TOF-MS of P(DHF-DMDOP$_{6.9}$) degradation product. **d** The photos of rectangle-shaped specimens of P(DHF-DMDOP$_{2.6}$) treated with camphorsulfonic acid solution after different degradation times. **e** The SEC profiles of accelerated degradation of oligomer. **f** The molecular weight change of oligomer during accelerated oxidative degradation.

lower for the PDHF copolymer samples [P(DHF-DMDOP$_{2.6}$) 122 °C, P(DHF-DMDOP$_{3.6}$) 112 °C and P(DHF-DMDOP$_{6.9}$) 100 °C, respectively] relatively to pure PDHF (131 °C) (Fig. 5a). Almost the same thermal decomposition temperature at 5% mass loss ($T_{d,5\%}$) of 332 °C was observed for P(DHF-DMDOP$_{2.6}$), and virgin PDHF prepared under identical conditions (Fig. 5b).

Giving the thermal properties of P(DHF-DMDOP$_{2.6}$) was similar to virgin PDHF and that this sample involved the lowest cleavable comonomer loading, we investigated its mechanical properties using tensile test. Compression-molded dumbbell-shaped samples demonstrated the impressive toughness and durability, with ε_b~39.0% and σ_b~43.1 MPa (Fig. 5c). Importantly, the ε_b for P(DHF-DMDOP$_{2.6}$) was approximately two times high than that of virgin PDHF, showing that the copolymerization approach overcomes the brittleness of PDHF.

To evaluate the potential of this new materials in packaging applications, we prepared the free-standing films of P(DHF-DMDOP$_{2.6}$) for analysis. The produced uniform films displayed the impressive optical properties, with transmittance > 90% across visible wavelengths (380–700 nm), and refractive index$_{589nm}$ of 1.54, nearly identical to the values for pure PDHF (Fig. S23). The oxygen (O$_2$) and water vapor permeability of the high-molecular-weight P(DHF-DMDOP$_{2.6}$) were also evaluated. The pure PDHF exhibited O$_2$ permeability of 0.34 barrer and water vapor transmittance rate of ~ 1.88 g·mm·m^{-2}·day^{-1}, respectively. The P(DHF-DMDOP$_{2.6}$) exhibited comparable O$_2$ permeability of 0.35 barrer and water vapor transmittance rate of ~2.16 g·mm·m^{-2}·day^{-1} (Fig. 5d, e). Moreover, the polar groups on the polymer side chain may endow adhesive properties to PDHF. Though high T_g, the PDHF could also exhibits adhesive properties similar to hot glue. We prepared the adhesive specimens on a steel substrate by hot press for lap shear test and measured the adhesive strength of PDHF. We observed PDHF and PDHF copolymer exhibit adhesive strength

approximate ~5 MPa on steel substrate, which is comparable with commercial adhesives PVAc[51] (Fig. 5f).

In general, P(DHF-DMDOP$_{2.6}$) sample showed comparable thermomechanical, optical, barrier, and adhesive properties to virgin PDHF, indicating that statistical incorporation of low acetal sequence into PDHF does not have a significant impact on these important polymer performance.

Discussion

Access to in-chain functionalized vinyl polymers that are less persistent in the environment while possessing desirable material properties, has received tremendous research interest over the past decades. Thus, developing renewable, and easily degradable PDHF remains an important research goal. To date, however, this endeavor has been hindered by the limitations of current cationic copolymerization techniques.

Here, we have described an efficient anion-binding catalysis methodology to deliver on-demand degradable polymers via the cationic copolymerization of DHF with acetals. The anion-binding catalyst system is capable of promoting reversibly activating both different dormant species-such as those derived from DHF through vinyl-addition and cyclic acetal through ring-opening, which allows an even distribution of acetal along polymer chain to furnish readily deconstructable PDHF copolymers with high-molecular-weight and low dispersity. This copolymer can be completely hydrolyzed into structure-defined oligomers under mildly acidic conditions. Looking forward, this strategy may have numerous implications for polymer design. While we herein demonstrate this strategy primarily for PDHF, we expect it to apply broadly to other vinyl polymers synthesized using cationic polymerization. This methodology for the preparation of degradable vinyl polymers has several distinct advantages: (1) an even distribution of degradable sequences, which results in a complete polymer degradation into structure-defined oligomers. (2) facile and
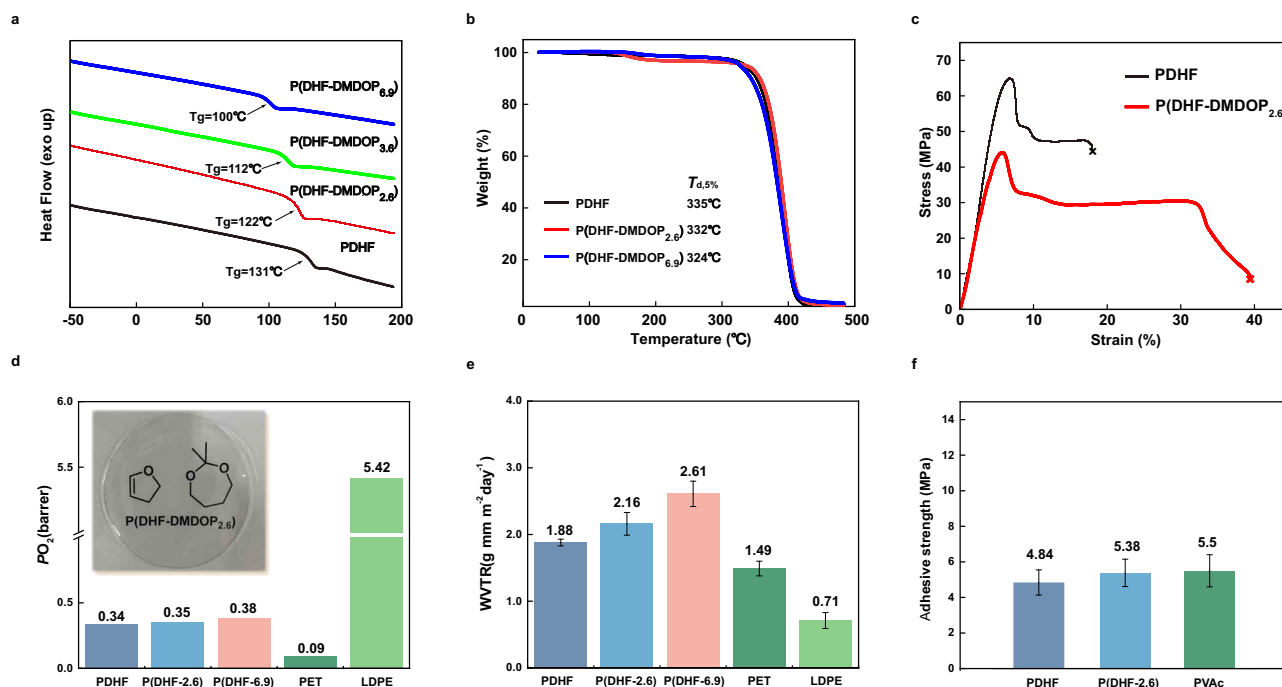
Fig. 5 | Physical properties of PDHF copolymers. a DSC curves of PDHF and P(DHF-*co*-DMDOP). **b** TGA curves of PDHF, P(DHF-DMDOP$_{2.6}$) and P(DHF-DMDOP$_{6.9}$). **c** Stress-strain curves of native PDHF (σ_{PDHF} = 64.9 MPa, ε_{PDHF} = 17.9%, $M_{n,MALLS}$ = 295.2 kg/mol) and P(DHF-DMDOP$_{2.6}$) (σ_b = 43.9 MPa, ε_b = 39.0%, $M_{n,MALLS}$ = 265.2 kg/mol). **d** PDHF copolymers showed comparable permeability for O$_2$ and **e** Water Vapor with native PDHF. Data are presented as mean ± SD (standard deviation) and collected from three independent experiments. The compared WVTR values for PET and LDPE were from recent article[9]. **f** Adhesive property comparison for PDHF and P(DHF-DMDOP$_{2.6}$). Data are presented as mean ± SD and collected from four independent experiments. The compared adhesive strength for PVAc was from reported article[51].

on-demand degradation under mild conditions. (3) both molecular weight control and high-molecular-weight. The new family of degradable copolymer accessed through the presented approach will find applications that range from degradable plastics to on-demand cleavaged adhesives.

Methods

Procedure for cationic copolymerization of DHF and cyclic acetals

In a nitrogen glovebox, polymerizations were set up in baked Schlenk glass tubes. A typical example of the polymerization procedure is given below. The cationic polymerization was initiated by addition of mixture of prechilled DHF (4 mmol, 300 μL) and DMDOP(0.8 mmol, 112 μL) via dry syringes into the solution containing seleno-cyclodiphosph(V)azanes (in DCM, 0.05 M, 10 μL),α-chloroisochroman (in DCM, 0.05 M, 10 μL), 1,2,3,4-tetrahydronaphthalene 20 μL as internal standard and DCM (70 μL) at −40 °C. The initial concentration [M]$_0$ of DHF in the reaction mixture was 8.0 M. The solution was stirred at −40 °C. After predetermined intervals, the reaction was terminated with prechilled methanol (0.20 mL) containing a small amount of Et$_3$N (5% (v:v) in MeOH) and diluted by DCM. The conversion was calculated by ^{1}H NMR analysis. To obtain isolated polymer, the solution was precipitated with methanol, and the resulting product was isolated by centrifugation and dried under vacuum for 24 h.

Procedure for the degradation of copolymer in homogeneous conditions

The degradation experiments were carried out by slow addition of 2 ml HCl aqueous solution (12 M) into the stirring THF solution (23 ml) containing poly(DHF-co-Acetal) (400 mg) at r.t. For GPC analysis, after predetermined intervals, aliquots were taken from the reaction mixture and precipitated into methanol, then centrifuged and dried under reduced pressure to afford the degradation product. For NMR and

MALDI-TOF-MS analysis, the reaction mixture was quenched with 20 ml saturated NaHCO$_3$ aqueous solution, then the organic phase was collected and dried under reduced pressure at 50 °C to afford the final degradation product.

Procedure for the degradation of copolymer in heterogeneous conditions

The copolymer specimens (40 mm × 15 mm, thickness ~ 0.15 mm) were immersed in the sealed vial containing the aqueous solution of 1.0 M camphorsulfonic acid (CSA) at room temperature. The M_n of sample was determined at predetermined dates.

Determination of molecular weight

For determining the M_ns of low-molecular-weight PDHF copolymer (Mn <50 kDa), Size Exclusion Chromatography (SEC) was conducted on a system composed of a Waters 2414 Refractive Index Detector equipped with a series of connected size exclusion columns (Styragel® HR 3 THF and Styragel® HR 4 THF, 300 × 7.8 mm, HPLC columns, Waters, USA). The system was operated with THF as the eluent at a flow rate of 1 mL/min at 35 °C and calibrated with PS standards.

The high-molecular-weight PDHF and PDHF copolymer samples were analyzed using a wyatt GPC-LS with PLgel MINED-B LS 300 × 7.5 mm chromatographic column at a flow rate of 1.000 mL/min (THF) at 25 °C. The high number-average molecular weights (M$_n$) and molecular weight distribution (Đ) for PDHF and PDHF-based copolymer were determined by light scattering using a Wyatt miniDawn Treos multi-angle light scattering detector and a dn/dc value of 0.1116 mL g^{-1}

Differential Scanning Calorimetry (DSC) analysis

DSC measurements, using ~5 mg of material, were performed on a TA Q2000 DSC-7 instrument under a N$_2$ atmosphere with a heating rate of 10 °C/min from −70 °C to 180 °C.

Thermal analysis

Thermogravimetric analysis (TGA) curves were obtained at a heating rate of 10 °C/min from 40 °C to 500 °C in N_2 with TGA-Q50 thermogravimetric analyzer. Thermal decomposition temperatures ($T_{d,5\%}$) were determined at 5% mass loss.

Tensile testing

For the tensile testing, the polymer was dissolved in DCM and 0.1 wt% Irganox 1010® was added, then evaporating over night before drying under vacuum at 70 °C for 24 h. The dog-bond-shape samples with approximate gauge dimensions of 16 × 4 x 1.0 mm were prepared by hot pressing. The polymer materials were held at 180 °C for 5 mins before pressing and then pressed into the mould and holding for another 5 minutes.

Tensile stress/strain tests were performed on a Zwiek/Z010 electronic universal testing machine at an elongation speed of 2 mm min^{-1} at room temperature.

Lap shear Testing

Polymer films (~10 mg) with a dimension of 12.5 mm × 10.0 mm were put between two steel sheets cut into 10 × 50 mm and were hot pressed at 180 °C for 5 mins and then cooled down with pressure to 25 °C for 20 mins. The specimens were kept at ambient condition for 1 day before test.

Test pieces for each sample were used to evaluate the adhesive strength using a Zwiek/Z010 electronic universal testing machine at 25 °C under a tensile speed of 10 mm/min at room temperature.

Measurement of Refractive Index

For ellipsometry, films of polymers were spin-coated onto silicon wafers. The thickness of films was measured by micro-profilometer.

The Ellipsometry was performed on a Senthech SE800 ellipsometer using wavelengths from 370 to 1000 nm with a 65° angle of incidence. The refractive index was predicted by the Cauchy dispersion equation.

Measurement of transmittance

UV/Vis absorption spectra were measured with a Shimadzu UV-3600 spectrometer. Polymer films were prepared by solvent evaporation (dichloromethane) and further dried on the vacuum at 50 °C for 24 h.

Measurement of water vapor transmission rate

The water vapor transmission measurement was performed on SYS-TESTER WVTR-255 according to cup method (ASTM-E96). For the measurement of Water Vapor Transmission Rate, films were prepared by solvent evaporation and further dried on the vacuum at 50 °C for 24 h. The thickness of films measured by micrometer caliper was ~68 μm.

Data availability

The size exclusion chromatography raw data, nuclear magnetic resonance raw data and properties test data generated in this study Information and have been deposited in Figshare under accession code of [https://doi.org/10.6084/m9.figshare.28856174]. The remaining data necessary to support the conclusions of this paper are provided in the main text and the Supplementary Information. All data are available from the corresponding author upon request. Source data are provided with this paper.

References

1. MacLeod, M., Arp, H. P. H., Tekman, M. B. & Jahnke, A. The global threat from plastic pollution. *Science* **373**, 61 (2021).
2. Law, K. L. et al. The United States' contribution of plastic waste to land and ocean. *Sci. Adv.* **6**, eabd0288 (2020).
3. Geyer, R., Jambeck, J. R. & Law, K. L. Production, use, and fate of all plastics ever made. *Sci. Adv.* **3**, e1700782 (2017).
4. Lu, H. et al. Machine learning-aided engineering of hydrolases for PET depolymerization. *Nature* **604**, 662 (2022).
5. Conk, R. J. et al. Catalytic deconstruction of waste polyethylene with ethylene to form propylene. *Science* **377**, 1561 (2022).
6. Dong, Q. et al. Depolymerization of plastics by means of electrified spatiotemporal heating. *Nature* **616**, 488 (2023).
7. Arroyave, A. et al. Catalytic chemical recycling of post-consumer polyethylene. *J. Am. Chem. Soc.* **144**, 23280 (2022).
8. Xia, Q. et al. A strong, biodegradable and recyclable lignocellulosic bioplastic. *Nat. Sustain.* **4**, 627 (2021).
9. Sangroniz, A. et al. Packaging materials with desired mechanical and barrier properties and full chemical recyclability. *Nat. Commun.* **10**, 3559 (2019).
10. Wang, Y., Zhu, Y., Lv, W., Wang, X. & Tao, Y. Tough while recyclable plastics enabled by monothiodilactone monomers. *J. Am. Chem. Soc.* **145**, 1877 (2023).
11. Li, X.-L. et al. Dual recycling of depolymerization catalyst and biodegradable polyester that markedly outperforms polyolefins. *Angew. Chem. Int. Ed.* **62**, e202303791 (2023).
12. von Vacano, B. et al. Sustainable design of structural and functional polymers for a circular economy. *Angew. Chem. Int. Ed.* **62**, e202210823 (2023).
13. Rahimi, A. & García, J. M. Chemical recycling of waste plastics for new materials production. *Nat. Rev. Chem.* **1**, 0046 (2017).
14. Shieh, P. et al. Publisher Correction: Cleavable comonomers enable degradable, recyclable thermoset plastics. *Nature* **585**, E4 (2020).
15. Tang, S., Seidel, F. W. & Nozaki, K. High density polyethylenes bearing isolated in-chain carbonyls. *Angew. Chem. Int. Ed.* **60**, 26506 (2021).
16. Feist, J. D., Lee, D. C. & Xia, Y. A versatile approach for the synthesis of degradable polymers via controlled ring-opening metathesis copolymerization. *Nat. Chem.* **14**, 53 (2022).
17. Feist, J. D. & Xia, Y. Enol ethers are effective monomers for ring-opening metathesis polymerization: synthesis of degradable and depolymerizable Poly(2,3-dihydrofuran). *J. Am. Chem. Soc.* **142**, 1186 (2020).
18. An, T., Ryu, H. & Choi, T.-L. Living alternating ring-opening metathesis copolymerization of 2,3-Dihydrofuran to provide completely degradable polymers. *Angew. Chem. Int. Ed.* **62**, e202309632 (2023).
19. Liu, P. et al. Mechanically triggered on-demand degradation of polymers synthesized by radical polymerizations. *Nat. Chem.* **16**, 1184 (2024).
20. Tashiro, K., Akiyama, M., Kashiwagi, K. & Okazoe, T. The Fluorocarbene exploit: enforcing alternation in ring-opening metathesis polymerization. *J. Am. Chem. Soc.* **145**, 2941 (2023).
21. Sanda, F. & Matsumoto, M. Degradation behavior of poly(2,3-dihydrofuran). *J. Appl. Polym. Sci.* **59**, 295 (1996).
22. Dimroth, P. & Pasedach, H. 2.3-Dihydrofurane. *Angew. Chem.* **72**, 865 (1960).
23. Spring, S. W. et al. Poly(2,3-Dihydrofuran): A strong, biorenewable, and degradable thermoplastic synthesized via room temperature cationic polymerization. *J. Am. Chem. Soc.* **144**, 15727 (2022).
24. Watanabe, H. & Kamigaito, M. Direct radical copolymerizations of thioamides to generate vinyl polymers with degradable thioether bonds in the backbones. *J. Am. Chem. Soc.* **145**, 10948 (2023).
25. Uchiyama, M., Murakami, Y., Satoh, K. & Kamigaito, M. Synthesis and degradation of vinyl polymers with evenly distributed thioacetal bonds in main chains: Cationic DT copolymerization of vinyl ethers and cyclic thioacetals. *Angew. Chem. Int. Ed.* **62**, e202215021 (2023).

26. Čamdžić, L. & Stache, E. E. Controlled radical polymerization of acrylates and isocyanides installs degradable functionality into novel copolymers. *J. Am. Chem. Soc.* **145**, 20311 (2023).

27. Albanese, K. R., Morris, P. T., Read de Alaniz, J., Bates, C. M. & Hawker, C. J. Controlled-radical polymerization of α-lipoic acid: a general route to degradable vinyl copolymers. *J. Am. Chem. Soc.* **145**, 22728 (2023).

28. Wang, W., Rondon, B., Wang, Z., Wang, J. & Niu, J. Macrocyclic Allylic sulfone as a universal comonomer in organocatalyzed photocontrolled radical copolymerization with vinyl monomers. *Macromolecules* **56**, 2052 (2023).

29. Hill, M. R. et al. Radical ring-opening copolymerization of cyclic ketene acetals and maleimides affords homogeneous incorporation of degradable units. *ACS Macro Lett.* **6**, 1071 (2017).

30. Baur, M., Lin, F., Morgen, T. O., Odenwald, L. & Mecking, S. Polyethylene materials with in-chain ketones from nonalternating catalytic copolymerization. *Science* **374**, 604 (2021).

31. Morgen, T. O., Baur, M., Göttker-Schnetmann, I. & Mecking, S. Photodegradable branched polyethylenes from carbon monoxide copolymerization under benign conditions. *Nat. Commun.* **11**, 3696 (2020).

32. Aoshima, S. & Kanaoka, S. A renaissance in living cationic polymerization. *Chem. Rev.* **109**, 5245 (2009).

33. Uchiyama, M., Satoh, K. & Kamigaito, M. Cationic RAFT and DT polymerization. *Prog. Polym. Sci.* **124**, 101485 (2022).

34. Wu, L. et al. Regulating cationic polymerization: From structural control to life cycle management. *Prog. Polym. Sci.* **145**, 101736 (2023).

35. Ishido, Y., Kanazawa, A., Kanaoka, S. & Aoshima, S. Controlled cationic alternating copolymerization of various enol ethers and benzaldehyde derivatives: Effects of enol ether structures. *J. Polym. Sci., Part A: Polym. Chem.* **52**, 1334 (2014).

36. Li, M. et al. Anion-binding catalysis enables living cationic polymerization. *Nat. Synth.* **1**, 815 (2022).

37. Li, M., Li, H., Zhang, X., Wang, X. & Tao, Y. Mechanistic insight into anion-binding catalytic living cationic polymerization. *Angew. Chem. Int. Ed.* **62**, e202303237 (2023).

38. Hufendiek, A., Lingier, S. & Du Prez, F. E. Thermoplastic polyacetals: chemistry from the past for a sustainable future? *Polym. Chem.* **10**, 9 (2019).

39. Hillmyer, M. A. The promise of plastics from plants. *Science* **358**, 868 (2017).

40. Maruyama, K., Kanazawa, A. & Aoshima, S. Controlled cationic copolymerization of vinyl monomers and cyclic acetals via concurrent vinyl-addition and ring-opening mechanisms: the systematic study of structural effects on the copolymerization behavior. *Polym. Chem.* **10**, 5304 (2019).

41. Qiu, H., Yang, Z., Köhler, M., Ling, J. & Schacher, F. H. Synthesis and Solution Self-Assembly of Poly(1,3-dioxolane). *Macromolecules* **52**, 3359 (2019).

42. Zhang, X., Zhang, C. & Zhang, X. A facile and unprecedented route to a library of thermostable formaldehyde-derived polyesters: highly active and selective copolymerization of cyclic acetals and anhydrides. *Angew. Chem. Int. Ed.* **61**, e202117316 (2022).

43. Lefay, C. & Guillaneuf, Y. Recyclable/degradable materials via the insertion of labile/cleavable bonds using a comonomer approach. *Prog. Polym. Sci.* **147**, 101764 (2023).

44. Okada, M. & Yamashita, Y. Cationic copolymerization of cyclic formals and vinyl ethers. *Makromol. Chem.* **126**, 266 (1969).

45. Okada, M., Yamashita, Y. & Ishii, Y. Cationic copolymerization of 1,3-dioxolane with styrene. *Makromol. Chem.* **94**, 181 (1966).

46. Shirouchi, T., Kanazawa, A., Kanaoka, S. & Aoshima, S. Controlled cationic copolymerization of vinyl monomers and cyclic acetals via concurrent vinyl-addition and ring-opening mechanisms. *Macromolecules* **49**, 7184 (2016).

47. Maruyama, K., Kanazawa, A. & Aoshima, S. Alternating cationic copolymerization of vinyl ethers and aryl-substituted cyclic acetals: structural investigation of effects of cyclic acetals on copolymerizability. *Macromolecules* **55**, 4034 (2022).

48. Hester, H. G., Abel, B. A. & Coates, G. W. Ultra-high-molecular-weight Poly(Dioxolane): Enhancing the mechanical performance of a chemically recyclable polymer. *J. Am. Chem. Soc.* **145**, 8800 (2023).

49. Abel, B. A., Snyder, R. L. & Coates, G. W. Chemically recyclable thermoplastics from reversible-deactivation polymerization of cyclic acetals. *Science* **373**, 783 (2021).

50. Kelen, T. & Tüdős, F. A new improved linear graphical method for determing copolymerization reactivity ratios. *React. Kinet. Catal. Lett.* **1**, 487 (1974).

51. Matos-Pérez, C. R., White, J. D. & Wilker, J. J. Polymer composition and substrate influences on the adhesive bonding of a biomimetic, cross-linking polymer. *J. Am. Chem. Soc.* **134**, 9498 (2012).

Acknowledgements

Author contributions

Y.T. and X.W. conceived the project and directed research. Z.Z. designed and conducted experiments and analyzed the results. Z.Z. and Y.T. wrote the initial manuscript. Z.Z., W.L., M.L., Y.W. revised subsequent versions of the manuscript. Y.T. edited the initial draft, and all authors contributed to drafting various sections of the manuscript and reviewed the entire manuscript.

Competing interests

The authors declare no competing interests.

Additional information

Supplementary information The online version contains supplementary material available at https://doi.org/10.1038/s41467-025-59834-8.

Correspondence and requests for materials should be addressed to Xianhong Wang or Youhua Tao.

Peer review information *Nature Communications* thanks the anonymous reviewers for their contribution to the peer review of this work. A peer review file is available.

Reprints and permissions information is available at http://www.nature.com/reprints

Publisher's note Springer Nature remains neutral with regard to jurisdictional claims in published maps and institutional affiliations.